Korean J. Chem. Eng., 40(11), 2724-2734 (2023)
DOI: 10.1007/s11814-023-1508-x

pISSN: 0256-1115
eISSN: 1975-7220

Thermotropic liquid crystalline 4-(Nonyloxy) benzoic acid: Phase transition temperatures, thermodynamic characterization, and separation of structural isomers

Birol Isik, Fatih Cakar, Husnu Cankurtaran, and Ozlem Cankurtaran†

Department of Chemistry, Faculty of Arts & Sciences, Yildiz Technical University, Esenler, Istanbul, 34220, Turkey
(*Received 17 January 2023 • Revised 24 May 2023 • Accepted 1 June 2023*)

Abstract−The retention behavior of various organic probes on the 4-(Nonyloxy) benzoic acid liquid crystal, which is used as a stationary phase, was investigated using the inverse gas chromatography method at infinite dilution. The thermodynamic parameters including the Flory-Huggins parameter, equation-of-state interaction parameter, the mole fraction activity coefficient, the effective exchange energy parameter, and residual thermodynamic parameters were determined in the temperature range of 423.15-433.15 K by using the retention behavior of the probes on the liquid crystal. It was determined from the thermodynamic parameters that all probes were poor solvents for the liquid crystal. Besides, the results of the 4-(Nonyloxy) benzoic acid liquid crystal was compared with a liquid crystal in the literature, and the effect of the number of alkyl groups on the liquid crystals on the Flory-Huggins interaction parameter and isomer separation was evaluated.

Keywords: 4-(Nonyloxy) Benzoic Acid, Phase Transitions, Liquid Crystal, Inverse Gas Chromatography, Thermodynamic Parameters, Isomer Separation

INTRODUCTION

The term "liquid crystal" (LC) can be expressed as interphase in aggregated form between a crystalline solid and isotropic liquid form. This intermediate phase is also called mesophase. LCs in this form may show anisotropic properties in some cases, while in some cases they may also show fluid properties as in isotropic liquids. Organic molecules, some micellar structures, and polymeric molecules can exhibit LC properties [1]. LCs have been widely used in various fields since the 1960s. LCs can be used in many devices and instruments such as displays, thermometers, optical instruments, medical devices, and sensors [2-4].

Thermotropic LCs are highly functional materials that can show different phase transitions depending on temperature and can be used in many devices such as liquid crystal displays (LCDs), optic devices, sensors, switchable light panels, and thermal mapping due to this feature. To diversify the usage fields of thermotropic LCs and to determine the most suitable fields, it is extremely important to determine the phase transition temperatures, the dissolution behavior in various solvents, the physicochemical properties such as the solubility parameters, and the enthalpy of dissolution [5-7].

As a characterization method, inverse gas chromatography (IGC) is simple, cost-effective, and highly accurate. The materials such as polymers, LCs, ionic liquids, and pharmaceutical materials, whose physicochemical properties will be determined in the IGC method, are filled into a chromatographic column in which various solvents with certain properties are injected [8-12]. As a result of phase transitions in materials, the existing stationary phase is replaced by a new stationary phase. These phase transitions and phase transition temperatures can be determined by passing volatile compounds over the existing stationary phase according to the IGC method [13, 14]. The thermodynamic properties of a material can be studied in the temperature range where that material completely transitions to the liquid phase, called the thermodynamic region. Interactions between the stationary phase and probe molecule can be evaluated by Flory-Huggins and equation-of-state interaction theories [15-17]. At infinite dilution, the specific retention volume, important properties of real solutions in polymer phases, can be correlated with the activity coefficient (γ_1^∞). This parameter is defined as the ratio of activity (a_1) and mole fraction (x_1). The γ_1^∞ value was obtained for gas-liquid chromatography, i.e., for relatively low molecular mass molecules such as the LC of the stationary phase. Therefore, it is appropriate to use it to explain the LC solvent interaction [18-20].

Since series of structural isomers have different molecular arrangements, they can have different toxicity and can be used in various industrial applications. Therefore, it is extremely important to distinguish structural isomers from each other to diversify their application areas and evaluate their toxicity. Various stationary phases can be used to separate structural isomers. Especially when LCs are used as stationary phases, a much more effective separation can be achieved compared to other stationary phases [21-23].

The aim of this study is to investigate the effect of the number of alkyl groups in the structure of LC molecules on the thermodynamic properties of LC. Thermodynamic properties of various LCs by the IGC method have been studied in the literature [24,25]. The novelty of this study is the comparison of thermodynamic properties depending on the increase in the number of alkyl chains in the LC structure. In this study, the thermodynamic properties of 4-(Nonyloxy) benzoic acid (NBA) LC were investigated with the IGC method at infinite dilution. First, phase transition temperatures were

†To whom correspondence should be addressed.
E-mail: kurtaran90@yahoo.com, kurtaran@yildiz.edu.tr

determined by differential scanning calorimetry (DSC) analysis and IGC experiments. After the determination of the thermodynamic region from the retention diagrams, the interactions between the LC and probe molecules were evaluated according to the Flory-Huggins and equation-of-state interaction theories, and the thermodynamic parameters were calculated. Isomer separation studies on the NBA LC stationary phase were carried out using the isomer series of various solvents.

EXPERIMENTAL

1. Materials and Methods

The chemical name, abbreviation, CAS number, source, mass fraction purity, purification method, analysis method, and molecular weight of all chemicals used in this study are listed in Table S1. NBA LC was used as a stationary phase in this study. Chromosorb W (AW-DMCS-treated, 80/100 mesh) was acquired from Sigma Aldrich and used as column filler material. Silane-treated glass wool and stainless-steel chromatographic column (1/8" o.d., 2.10 mm i.d. 10 m) were acquired from Alltech Associates Inc.

All measurements in IGC studies at infinite dilution were performed by Agilent Technologies HP-6890N gas chromatography device combined with a thermal conductivity detector (TCD). Phase transition temperatures of NBA LC were determined by a differential scanning calorimeter Perkin Elmer DSC4000 under non-isothermal conditions. The sample (5 mg) was placed in a standard open aluminum pan and the analysis was performed under inert nitrogen gas with a flow rate of 20 mL·min^{-1} that did not react with the substance. The measurements were performed at 283.15 K·min^{-1} heating and cooling rate in the temperature range of 350.15-430.15 K and heat flow calibration in the temperature range between 223.15 and 698.15 K using seven different samples (Mercury, Cyclopentane, Gallium, Indium, Lead, Tin, and Zinc). The phase transition temperatures were determined as onset temperatures from DSC curves. Optical investigations of this LC were performed by a Mettler FP-82 HT hot stage and a control unit in conjunction with a Leica DM2700P polarizing microscope and Leica DMC2900 digital camera. The associated enthalpies were obtained from DSC-thermograms.

2. The Preparation of the Chromatographic Column

Before the preparation of NBA as a stationary phase, it was kept in a vacuum oven at 333.15-343.15 K for 48 h to remove excess moisture. Likewise, Chromosorb W (AW-DMCS-treated, 80/100 mesh) column filler material was kept in a vacuum oven at 378.15 K for 48 h. NBA LC was dissolved in chloroform and Chromosorb W (AW-DMCS-treated, 80/100 mesh) column filler material was added slowly with continuous stirring. The solvent of the obtained homogeneous mixture was slowly evaporated on a water bath heater and the stationary phase was obtained as a powder. It was confirmed that the Chromosorb W (AW-DMCS-treated, 80/100 mesh) did not adsorb any solvent before measurements. The eluted peaks of studied solvents were sharp, symmetrical, and reproducible. The retention times were precise and reproducible to ±0.001 min. The resulting powder product was dried in a vacuum oven at 333.15-343.15 K for 48 h. A burn test was carried out with some of this product and the amount of LC coated on Chromosorb W (AW-DMCS-treated, 80/100 mesh) was found to be 10.8%. Approximately 1.2 g of the prepared stationary phase was loaded into a 1 m stainless-steel column. The column ends were loosely plugged with silanized glass wool. The prepared chromatographic column was placed in the device and conditioning was carried out at 393.15 K for 24 h under Helium (He) atmosphere. Afterward, IGC experiments were carried out under He atmosphere with a flow rate of 3.6 mL·min^{-1}. The flow rate of the carrier gas was kept below 6 mL·min^{-1}. It was determined experimentally that the retention volume was independent of the flow rate of the carrier gas below this rate and eluted peaks were sharp and reproducible [26]. Polar and non-polar probes were passed over the stationary phase using a 1 μL Hamilton syringe, and their retention behavior was examined. Likewise, a 10 μL Hamilton syringe was used to obtain the air peak. For infinite dilution, the solvent (0.1 μL) was taken into the syringe and flushed into the air. Then, the retention times for solvent and air were determined. During the IGC analysis, the temperature values in the gas outlet section of the IGC device were recorded as the ambient temperature. For the accuracy of experimental data, at least four consecutive injections were made for each probe and air at each set of measurements. The retention time was calculated as the average of four experiments.

RESULTS AND DISCUSSION

1. The Determination of Phase Transition Temperatures

The phase transition temperatures of LCs can be easily determined by both DSC analysis and IGC experiments. These temperatures of the NBA LC were determined by performing the DSC analysis in the temperature range of 343.15-433.15 K, with the heating and cooling rate set to 283.15 K·min^{-1}. The DSC curves and textures of the nematic and smectic phase are given in Fig. 1. When Fig. 1 was examined, it was determined that the phase transition temperatures were 365.55, 390.85, and 416.85 K and the phase transition enthalpies were 33.18, 1.54, and 1.75 kJ·mol^{-1}. Besides, the phase transition temperatures and enthalpies of NBA LC are listed in Table 1. According to Tejaswi et al., the peaks at 362.25, 385.75, and 407.15 K correspond to solid I to smectic C phase, smectic C to nematic phase, and nematic to isotropic phase, respectively in the cooling stage. According to this work, the phase transition enthalpies were determined as 6.18, 0.92, and 0.32 kJ·mol^{-1} at the cooling stage [27]. According to Kumar et al., the peaks at 365.45, 386.25, and 415.05 K correspond to crystalline to smectic C phase, smectic C to nematic phase, and nematic to isotropic phase, respectively, on heating. The phase transition enthalpies were found as 28.71, 0.97, and 1.75 kJ·mol^{-1} at the heating stage [7]. According to Herbert, the peaks at 365.15, 391.15, and 418.15 K correspond to solid to smectic phase, smectic to nematic phase, and nematic to isotropic phase. The phase transition enthalpies were found as 33.47, 1.67, and 2.51 kJ·mol^{-1} at the heating stage [28]. In this study, the phase transition temperatures and enthalpies obtained as a result of DSC analysis were compatible with the values in the literature.

The phase transition temperatures of the NBA LC were also determined by the IGC method at infinite dilution. For this, n-butyl acetate (nBAc), n-butyl alcohol (nBAl), and n-amyl alcohol (nAAl) probes were passed over the stationary phase at a tempera-

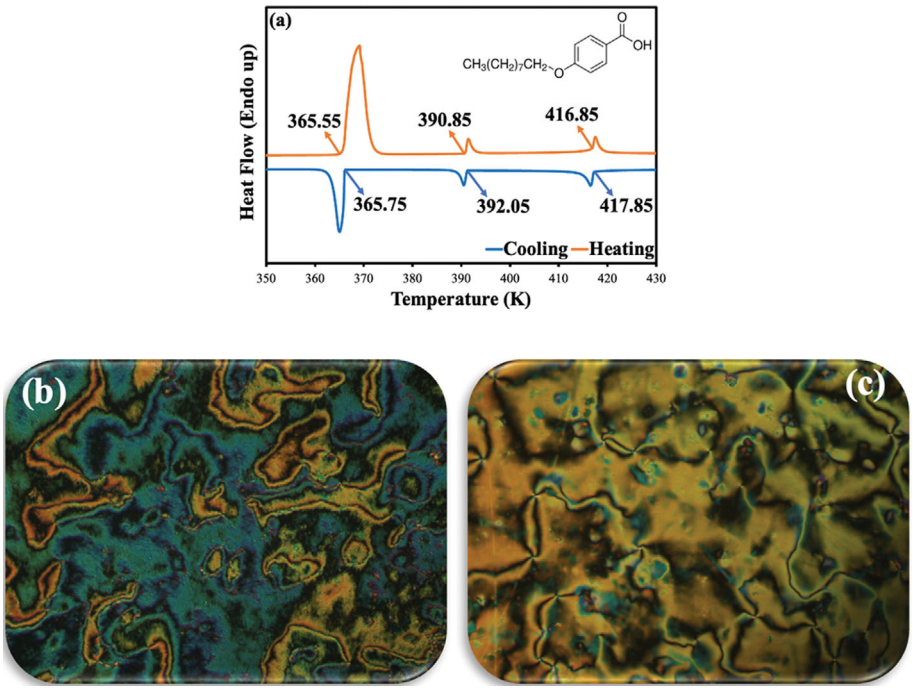

Fig. 1. DSC curves of NBA LC at heating and cooling stage (283 K·min^{-1}) (a) and the texture of the N (412.95 K) (b) and SmC (371.35 K) (c) phase on cooling

Table 1. The phase transition temperatures and enthalpies of NBA LC on heating and cooling cycle

Parameters		Heating			Cooling		
Transition type	Ref.	Cr - SmC	SmC - N	N - Iso	SmC - Cr	N - SmC	Iso - N
Phase transition temperatures (K)	This work[a]	365.55	390.85	416.85	366.75	392.05	417.85
	[7]	365.45	386.25	415.05	358.55	383.55	413.15
	[27]	-	-	-	362.25	385.75	407.15
	[28]	365.15	391.15	418.15	-	-	-
Enthalpies (ΔH, kJ·mol^{-1})	This work[b]	33.18	1.54	1.75	10.02	1.30	1.33
	[7]	28.71	0.97	1.75	8.19	0.86	1.90
	[27]	-	-	-	6.18	0.92	0.32
	[28]	33.47	1.67	2.51	-	-	-

Cr: Crystalline solid phase, SmC: Smectic C phase, N: Nematic phase, Iso: Isotropic liquid phase. The measurements were performed at 10 °C/min heating and cooling rate. The experiments were made under average atmospheric pressure (101.56 kPa), u(P)=0.26 kPa.
[a]Standard uncertainty in the phase transition temperatures, which are derived from the DSC data, are estimated to be ±0.35 K.
[b]Standard uncertainty in enthalpies, which are derived from the DSC data, are estimated to be 0.36 kJ·mol^{-1}.

ture range of 303.15-433.15 K, and their retention behavior was investigated. The interactions between the LC and probe molecule can be examined using the specific retention volume (V_g^o). Using the retention data obtained as a result of this process, V_g^o values were calculated with the help of Eq. (1) [29-31], and retention diagrams were drawn (Fig. 2). When Fig. 2 was examined, it was determined that the NBA LC exhibited three-phase transition temperatures (365.15, 387.15, and 405.15 K). It was determined that the phase transition temperatures obtained as a result of the IGC experiments were compatible with the phase transition temperatures obtained by DSC analysis and the literature. According to Fig. 2, the thermodynamic region was determined as 423.15-433.15 K from the retention diagrams.

$$V_g^o = \frac{Q * J * (t_R - t_A) * 273.15}{T_f * w} \quad (1)$$

where Q is the volume of mobile phase passing per minute, t_A and t_R are the retention time of air and probe molecule on the stationary phase, respectively, w is the total mass of the LC loaded as the stationary phase to the chromatographic column, T_f is the ambient temperature and J is the pressure correction factor calculated according to the $J=[3(p_i/p_o)^2-1]/[2(p_i/p_o)^3-1]$. In this equation, p_i is the pressure at the column inlet, and p_o is the pressure at the column outlet [32,33].

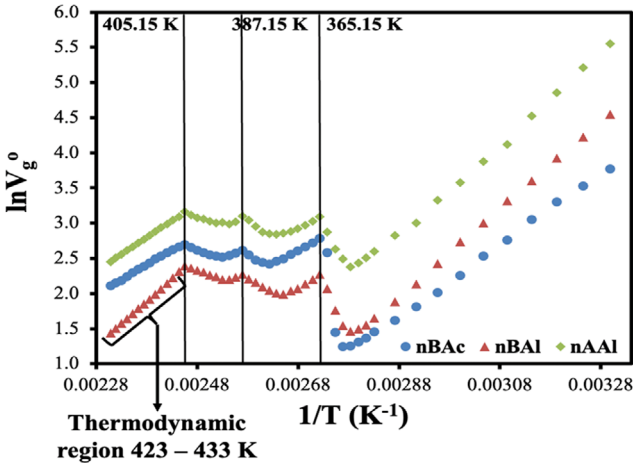

Fig. 2. The retention diagrams of nBAc, nBAl, and nAAl probes on NBA LC.

2. Thermodynamic Characterization

The LC-probe molecule interaction was examined from the V_g^o values calculated according to Eq. (1). In the thermodynamic region (423.15-433.15 K), non-polar and polar probes were passed over the stationary phase and their retention behavior was investigated. Also, linear retention diagrams were drawn for non-polar and polar probes. With the linear retention diagrams in Fig. 3, thermodynamic parameters were calculated according to different theories.

2-1. Flory-Huggins and Equation-of-state Interaction Parameters

The interactions between the LC and the probe molecule and the solubility behavior of the LC can be studied with the Flory-Huggins and equation-of-state interaction theories [9,34-36]. Although still valid, Flory-Huggins is insufficient to explain the concentration dependence of χ and the negative volume changes in the mixture due to mixing of chain molecules. During the middle 1960's Flory introduced a theory of solutions that stresses the importance of the equation-of-state theory properties of the pure components for determining the thermodynamic properties of their solutions. In the theory, a pure solvent is described with a partition function. By differentiation, it yields the equation of state for pure components and their mixtures, which can be expressed in a reduced form [37]. According to these theories, the Flory-Huggins interaction parameter (χ_{12}^{∞}) and equation-of-state interaction parameter (χ_{12}^{*}) for LC were calculated with the help of Eqs. (2) and (3) for different temperatures (423.15-433.15 K) and non-polar and polar probes and are listed in Table 2 and 3.

$$\chi_{12}^{\infty}=\ln\left(\frac{273.15*R*v_2}{V_g^o*P_1^o*V_1^o}\right)-\left(1-\frac{V_1^o}{M_2*v_2}\right)-\left(\frac{P_1^o*(B_{11}-V_1^o)}{R*T}\right) \quad (2)$$

$$\chi_{12}^{*}=\ln\left(\frac{273.15*R*v_2^*}{V_g^o*P_1^o*V_1^*}\right)-\left(1-\frac{V_1^o}{M_2*v_2^*}\right)-\left(\frac{P_1^o*(B_{11}-V_1^o)}{R*T}\right) \quad (3)$$

Here, R is the ideal gas constant, P_1^o is the vapor pressure of the probe molecule, V_1^o is the molar volume of the probe molecule, M_2 is the molecular weight of the LC molecule, T is the column temperature, v_2 and v_2^* are the specific and characteristic volume of the LC molecule, V_1^* is the characteristic molar volume of probe molecule, and B_{11} is the second virial coefficient of the deviation of the vapor phase solvent from the ideality and can be calculated as follows:

$$B_{11}=\frac{(0.430-0.886(T_c/T)-0.694(T_c/T)^2-0.037(n-1)(T_c/T)^{9/2})}{V_c} \quad (4)$$

Here, n is the number of carbon atoms in solvents (for permanent gases, n=1 and the last term becomes zero); T_c is the critical temperature of the solvents and V_c is the critical molar volume of the solvents [38,39].

Flory-Huggins theory assumes that probes are poor for LC when χ_{12}^{∞} values are greater than 0.5, good solvents when less than 0.5, and moderate solvents when equal to 0.5 [40,41]. According to this assumption, when Table 2 was examined, it was determined that all non-polar and polar probes were poor solvents for NBA LC in the temperature range of 423.15-433.15 K. The high χ_{12}^{*} values also supported the χ_{12}^{∞} values. Besides, it was observed that these values increased and the solubility decreased with increasing temperature. It is known that heat energy is released in exothermic reactions when the solute is dissolved in a solvent, and as a result of the heat energy released, the interaction between the solvent and the solute decreases. In this case, it is possible to say that

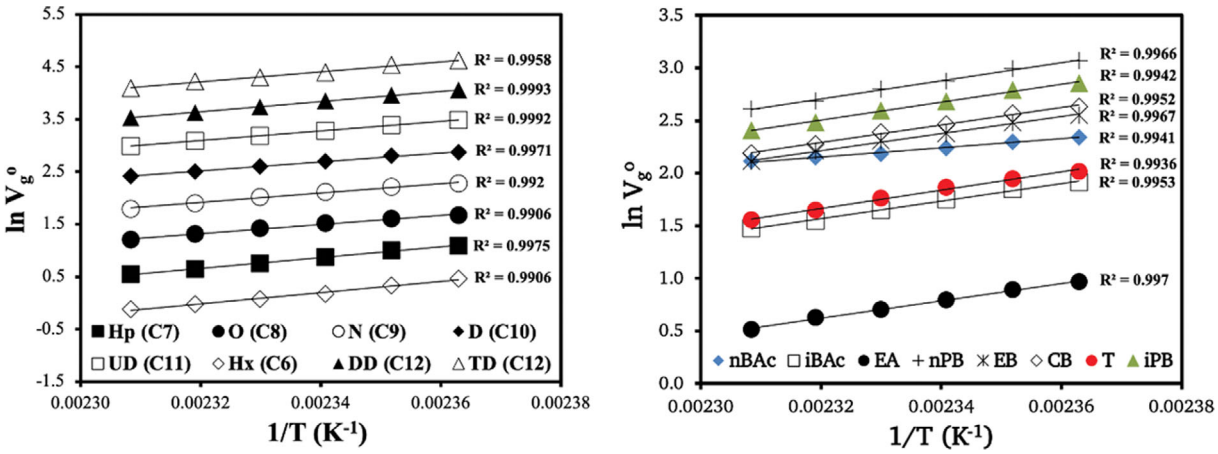

Fig. 3. The retention diagrams of non-polar and polar probes on NBA LC.

Table 2. The Flory-Huggins interaction parameters (χ_{12}^{∞}) of the probes with NBA LC

Temperature (K)	423.15	425.15	427.15	429.15	431.15	433.15
$p_i - p_o$ (kPa)[a]	46.53	47.83	49.46	50.39	51.01	51.84
Probes	Flory-Huggins interaction parameters (χ_{12}^{∞})					
Hx (C6)	2.38	2.48	2.61	2.67	2.74	2.81
Hp (C7)	2.37	2.41	2.51	2.59	2.66	2.72
O (C8)	2.39	2.41	2.46	2.51	2.58	2.64
N (C9)	2.39	2.40	2.46	2.51	2.57	2.64
D (C10)	2.40	2.42	2.47	2.52	2.56	2.60
UD (C11)	2.40	2.43	2.49	2.52	2.56	2.60
DD (C12)	2.43	2.47	2.51	2.56	2.61	2.64
TD (C13)	2.48	2.50	2.56	2.59	2.60	2.66
nBAc	1.75	1.75	1.76	1.77	1.76	1.76
iBAc	1.97	1.99	2.04	2.10	2.16	2.19
EA	2.07	2.11	2.17	2.23	2.26	2.34
nPB	1.87	1.89	1.96	1.99	2.05	2.08
iPB	1.86	1.87	1.94	1.98	2.04	2.07
EB	1.85	1.88	1.94	1.96	2.01	2.06
CB	1.75	1.76	1.82	1.85	1.92	1.97
T	1.69	1.72	1.76	1.82	1.90	1.95

Standard uncertainty u is $u(\chi_{12}^{\infty})=0.03$; u(T)=0.10 K; u(P)=0.26 kPa.
[a]p_i: inlet pressure, p_o: outlet pressure

Table 3. The equation-of-state interaction parameters (χ_{12}^{*}) of the probes with NBA LC

Temperature (K)	423.15	425.15	427.15	429.15	431.15	433.15
$p_i - p_o$ (kPa)[a]	46.53	47.83	49.46	50.39	51.01	51.84
Probes	Equation-of-state interaction parameters (χ_{12}^{*})					
Hx (C6)	2.44	2.54	2.67	2.73	2.80	2.87
Hp (C7)	2.44	2.43	2.52	2.60	2.67	2.73
O (C8)	2.37	2.39	2.43	2.49	2.55	2.62
N (C9)	2.34	2.35	2.41	2.46	2.52	2.58
D (C10)	2.33	2.34	2.39	2.44	2.48	2.52
UD (C11)	2.31	2.33	2.39	2.42	2.46	2.49
DD (C12)	2.31	2.35	2.39	2.44	2.48	2.51
TD (C13)	2.35	2.36	2.42	2.44	2.48	2.51
nBAc	1.78	1.78	1.79	1.80	1.79	1.78
iBAc	1.99	2.01	2.06	2.12	2.18	2.21
EA	2.18	2.21	2.28	2.33	2.37	2.45
nPB	1.86	1.88	1.95	1.97	2.04	2.06
iPB	1.85	1.86	1.93	1.96	2.03	2.05
EB	1.87	1.89	1.95	1.97	2.02	2.08
CB	1.77	1.79	1.85	1.88	1.95	1.99
T	1.73	1.76	1.81	1.87	1.94	2.00

Standard uncertainty u is $u(\chi_{12}^{*})=0.03$; u(T)=0.10 K; u(P)=0.26 kPa.
[a]p_i: inlet pressure, p_o: outlet pressure

the solubility of LC in non-polar and polar probes is exothermic.

To investigate the effect of the -CH_2 group number on thermodynamic parameters in LCs, the results were compared with those of 4-(Octyloxy) benzoic acid (OBA) given in our previous study [42]. It was assumed that the χ_{12}^{∞} values varied linearly with 1/T values [43,44]. Accordingly, linear diagrams (Fig. 4) were drawn for non-polar and polar probes between 1/T and χ_{12}^{∞} values. The χ_{12}^{∞} values of the NBA LC at 423.15-433.15 K were calculated by extrapolating from the linear graphs obtained and listed in Table 4. As the number of -CH_2 groups in the LC structure increases, the

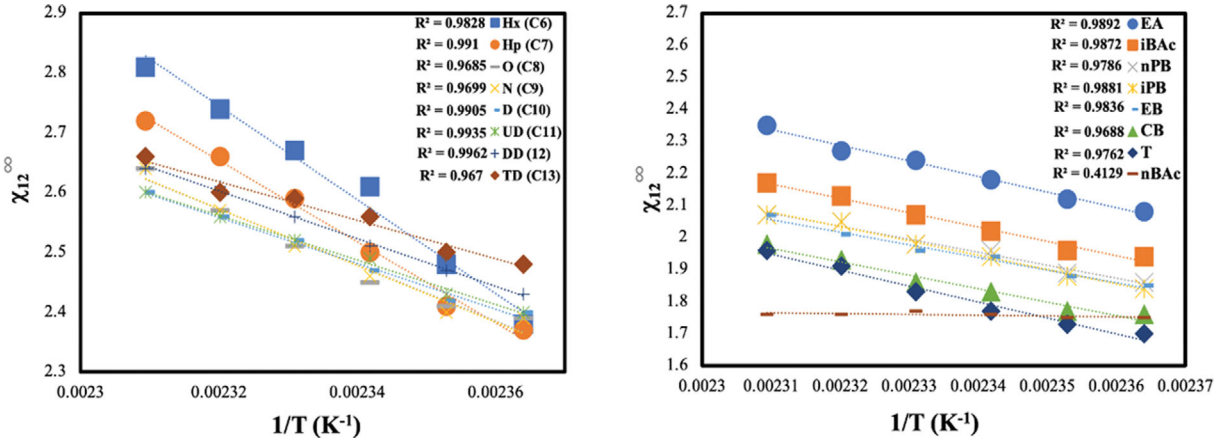

Fig. 4. The linear plots of 1/T and χ_{12}^{∞} values for non-polar and polar probes.

Table 4. The comparison of the Flory-Huggins interaction parameters (χ_{12}^{∞}) of the probes with OBA and NBA LC

	OBA LC [42]						NBA [This study]					
Temperature (K)	433.15	435.15	437.15	439.15	441.15	443.15	433.15	435.15	437.15	439.15	441.15	443.15
Probes	Flory-Huggins interaction parameters (χ_{12}^{∞})											
Hx (C6)	2.27	2.38	2.50	2.62	2.78	2.86	2.82	2.91	3.00	3.07	3.15	3.24
Hp (C7)	2.20	2.35	2.48	2.53	2.67	2.77	2.72	2.80	2.87	2.94	3.01	3.08
O (C8)	2.13	2.21	2.30	2.37	2.46	2.51	2.62	2.67	2.72	2.77	2.82	2.87
N (C9)	2.11	2.17	2.21	2.25	2.32	2.37	2.62	2.67	2.72	2.77	2.82	2.87
D (C10)	2.06	2.10	2.13	2.18	2.26	2.31	2.60	2.64	2.68	2.72	2.76	2.80
UD (C11)	2.05	2.08	2.10	2.15	2.19	2.22	2.60	2.64	2.68	2.72	2.76	2.80
DD (C12)	2.05	2.08	2.11	2.14	2.18	2.22	2.64	2.69	2.73	2.77	2.81	2.85
TD (C13)	2.09	2.12	2.13	2.15	2.19	2.29	2.65	2.69	2.72	2.75	2.79	2.82
nBAc	1.75	1.75	1.77	1.80	1.82	1.86	1.77	1.77	1.77	1.77	1.77	1.78
iBAc	1.81	1.84	1.86	1.88	1.90	1.91	2.17	2.22	2.27	2.31	2.36	2.40
EA	1.59	1.64	1.80	1.88	2.01	2.15	2.34	2.39	2.44	2.49	2.54	2.59
nPB	1.75	1.76	1.76	1.78	1.79	1.79	2.08	2.12	2.16	2.21	2.25	2.29
iPB	1.77	1.78	1.79	1.80	1.82	1.86	2.08	2.13	2.18	2.22	2.27	2.31
EB	1.68	1.74	1.76	1.78	1.82	1.87	2.06	2.10	2.14	2.18	2.22	2.27
CB	1.78	1.82	1.85	1.85	1.91	1.92	1.97	2.01	2.06	2.10	2.14	2.19
T	1.83	1.90	1.95	1.99	2.01	2.06	1.95	2.00	2.06	2.11	2.16	2.21

Standard uncertainty u is $u(\chi_{12}^{\infty})=0.07$; u(T)=0.10 K; u(P)=0.26 kPa.

χ_{12}^{∞} values increase and therefore the solubility decreases. In this case, when Table 4 was examined, it was found that the χ_{12}^{∞} values were greater for all probes in the NBA LC than in the OBA LC.

2-2. Mole Fraction Activity Coefficient at Infinite Dilution

The interactions between the probe molecule and NBA LC were investigated with the net retention volume (V_N). The V_N values were calculated from the following equation [45].

$$V_N = Q * J * (t_R - t_A)T/T_f \quad (4)$$

where Q is the volume of mobile phase passing in one minute, J is the James-Martin pressure correction factor, T and T_f are the column and ambient temperature (K), t_R and t_A are the retention time of probe molecules and air, respectively. Retention times were recorded as the average of four measurements to minimize error.

Using the V_N values, the mole fraction activity coefficient at infinite dilution (γ_1^{∞}) can be calculated with the following equation suggested by Everett [46] and Cruickshank [47].

$$\ln(\gamma_1^{\infty}) = \ln\left(\frac{n_2 * R * T}{V_N * P_1^o}\right) - \frac{P_1^o * (B_{11} - V_1^o)}{R * T} + \frac{P_o * J * (2B_{13} - V_1^{\infty})}{R * T} \quad (5)$$

where n_2 is the number of moles of the stationary phase, B_{13} is the mixed second virial coefficient of the probe molecule and mobile phase. Guillet et al. [48] indicated that the last term in Eq. (5) can be ignored at moderate mobile phase pressures (less than 202.65 kPa). In this situation, Eq. (5) was revised as the following equation [18-20,49-51].

$$\ln(\gamma_1^{\infty}) = \ln\left(\frac{n_2 * R * T}{V_N * P_1^o}\right) - \frac{P_1^o * (B_{11} - V_1^o)}{R * T} \quad (6)$$

This equation is commonly used for relatively low molecular

Table 5. The experimental values of the mole fraction activity coefficients at infinite dilution (γ_1^∞) different probes in NBA LC as a function of temperature; the solute standard state is hypothetical liquid at zero pressure

Temperature (K)	423.15	425.15	427.15	429.15	431.15	433.15
$p_i - p_o$ (kPa)[a]	46.53	47.83	49.46	50.39	51.01	51.84
Probes	Mole fraction activity coefficients (γ_1^∞)					
Hx (C6)	13.62	15.10	17.30	18.46	19.90	21.41
Hp (C7)	13.78	14.50	15.94	17.39	18.69	20.00
O (C8)	14.41	14.71	15.45	16.38	17.54	18.84
N (C9)	14.65	14.86	15.73	16.61	17.73	18.98
D (C10)	14.88	15.14	15.97	16.84	17.65	18.35
UD (C11)	14.93	15.41	16.33	16.99	17.69	18.45
DD (C12)	15.30	15.93	16.64	17.61	18.48	19.13
TD (C13)	16.00	16.34	17.46	18.05	18.27	19.44
nBAc	7.129	7.167	7.267	7.352	7.319	7.301
iBAc	8.903	9.119	9.653	10.26	10.92	11.34
EA	8.801	9.169	9.806	10.43	10.90	11.82
nPB	8.099	8.325	8.937	9.223	9.847	10.15
iPB	8.038	8.171	8.744	9.111	9.790	10.07
EB	7.573	7.812	8.310	8.536	9.031	9.578
CB	6.216	6.362	6.777	7.024	7.552	7.924
T	6.064	6.277	6.583	7.040	7.624	8.052

Standard uncertainty u is $u(\gamma_1^\infty)=\pm 3\%$; u(T)=0.10 K; u(P)=0.26 kPa.
[a]p_i: inlet pressure, p_o: outlet pressure

weight stationary phases. This equation also contains additional terms describing compressibility and the interaction of solute molecules with the mobile phase.

The γ_1^∞ values were determined from Eq. (6) and their values listed in Table 5. It can be seen clearly that the values of γ_1^∞ increase with enhancing the chain length of n-alkanes. As can be seen from Table 5, the solubility of NBA LC decreased with molecular weight. It can also be said that this situation results from the decrease in solubility as the chain length of the alkyl groups of aromatic hydrocarbons increases. The γ_1^∞ values of hydrocarbons were found to be greater than those of polar solvents. This is because hydrocarbons are non-polar solvents and interact weaker with polar LCs. It can be said that this interaction between the two structures arises from the long alkyl chains in the LC structure. This may also cause the solubility of the alkyl groups of hydrocarbons to decrease with increasing chain length [9,50]. It was also found that the γ_1^∞ values generally increased with increasing temperature, which indicates that the solubility of these solvents and all other solvents in NBA LC is exothermic.

The partial molar residual enthalpic ($\Delta\overline{H}_1^{E,\infty}$) and entropic ($\Delta\overline{S}_1^{E,\infty}$) components of the interaction at infinite dilution can be calculated from the slope and cut-off point of a linear plot between $\ln(\gamma_1^\infty)$ and 1/T values according to Eq. (7) [52].

$$\ln(\gamma_1^\infty)=\frac{\Delta\overline{H}_1^{E,\infty}}{RT}-\frac{\Delta\overline{S}_1^{E,\infty}}{R} \quad (7)$$

The residual partial molar heat ($\Delta\overline{H}_1^{E,\infty}$) and residual partial molar entropy ($\Delta\overline{S}_1^{E,\infty}$) of mixing were calculated from the slope and cut-off point of the linear plot drawn between $\ln(\gamma_1^\infty)$ and 1/T, respectively, according to Eq. (7) and their values listed in Table 6. The negative values of $\Delta\overline{H}_1^{E,\infty}$ for all of the studied probes refer to exothermic solubility. It can be determined that all the residual thermodynamic parameters ($\Delta\overline{H}_1^{E,\infty}$ and $\Delta\overline{S}_1^{E,\infty}$) have a negative sign and their absolute values increase with increasing solubility, that is, the smaller the γ_1^∞ value, the higher the absolute value of the residual thermodynamic parameters. The negative $\Delta\overline{H}_1^{E,\infty}$ values correspond to favorable interactions between NBA LC and probes at infinite dilution. Similarly, the negative $\Delta\overline{S}_1^{E,\infty}$ values imply that the solvents make the NBA LC more regular. However, since entropic contribution is higher than enthalpic contribution, the $\Delta\overline{G}_1^{E,\infty}$ values positive for all probes.

2-3. The Effective Exchange Energy Parameter

To evaluate the solubility of LC in non-polar and polar probes in addition to the χ_{12}^∞, χ_{12}^*, and γ_1^∞ parameters, the effective exchange energy parameter (χ_{eff}) is also widely used. The χ_{eff} values can be easily calculated using the χ_{12}^* values with the help of the following equation:

$$R*T*(\chi_{12}^*) = P_1^**V_1^**\left\{3*T_{1r}*\ln\left[\frac{(v_{1r}^{1/3}-1)}{(v_{2r}^{1/3}-1)}\right]+v_{1r}^{-1}-v_{2r}^{-1}+\frac{\chi_{eff}}{P_1^**v_{2r}}\right\} \quad (8)$$

Here, P_1^* is the characteristic pressure and v_{1r}, and v_{2r} are the reduced volume of the probe and LC molecules, respectively, and T_{1r} is the reduced temperature of the probe molecule.

The χ_{eff} values were calculated according to Eq. (8) and listed in Table 7. When χ_{eff} values are high, non-polar and polar probes are assumed to be poor solvents for LC [53]. In this case, when Table

Table 6. Values of partial molar residual Gibbs energy ($\Delta\overline{G}_1^{E,\infty}$), enthalpy ($\Delta\overline{H}_1^{E,\infty}$) and entropy ($\Delta\overline{S}_1^{E,\infty}$) of the probes for NBA LC at 423.15 K

Probes	$-\Delta\overline{H}_1^{E,\infty}$ (kJ·mol^{-1})	$-\Delta\overline{S}_1^{E,\infty}$ (J·mol^{-1}·K^{-1})	$\Delta\overline{G}_1^{E,\infty}$ (kJ·mol^{-1})
Hx (C6)	68.78	184.4	9.256
Hp (C7)	59.07	161.3	9.193
O (C8)	41.87	120.9	9.302
N (C9)	40.88	118.7	9.358
D (C10)	34.02	102.7	4.451
UD (C11)	32.93	100.3	9.500
DD (C12)	35.24	105.9	9.586
TD (C13)	29.26	92.20	9.742
nBAc	4.230	26.40	6.924
iBAc	39.65	111.8	7.640
EA	44.72	123.7	7.618
nPB	36.22	102.9	7.336
iPB	37.22	105.2	7.281
EB	35.61	100.9	7.094
CB	38.40	105.8	6.375
T	44.99	121.2	6.275

Standard uncertainty u is u($-\Delta\overline{H}_1^{E,\infty}$)=±0.6 kJ·mol^{-1}; u($-\Delta\overline{S}_1^{E,\infty}$)=±0.6 J·mol^{-1}·K^{-1}; u($\Delta\overline{G}_1^{E,\infty}$)=±0.6 kJ·mol^{-1}; u(T)=0.10 K; u(P)=0.26 kPa.

Table 7. The effective exchange energy parameters (χ_{eff}, J·cm^{-3}) of the probes with NBA LC

Temperature (K)	423.15	425.15	427.15	429.15	431.15	433.15
p_i-p_o (kPa)[a]	46.53	47.83	49.46	50.39	51.01	51.84
Probes	Effective exchange energy parameters (χ_{eff}, J·cm^{-3})					
Hx (C6)	79.31	83.85	89.84	92.87	96.35	99.79
Hp (C7)	67.71	69.69	73.36	76.73	79.58	82.38
O (C8)	60.82	61.57	63.26	65.27	67.64	70.13
N (C9)	53.76	54.22	55.96	57.64	59.64	61.78
D (C10)	49.65	50.15	51.64	53.13	54.46	55.58
UD (C11)	45.39	46.19	47.67	48.69	49.73	50.83
DD (C12)	42.59	43.52	44.56	45.89	46.73	47.88
TD (C13)	39.68	40.15	41.59	42.33	43.62	44.00
nBAc	50.19	50.35	50.88	51.31	51.08	50.93
iBAc	57.51	58.48	60.80	63.30	65.99	67.48
EA	87.92	90.33	94.24	97.88	100.6	105.3
nPB	54.90	55.93	58.60	59.80	62.30	63.49
iPB	55.24	55.85	58.41	59.98	62.73	63.84
EB	63.59	64.93	67.62	68.81	71.30	73.92
CB	74.54	75.74	79.01	80.89	84.68	87.25
T	66.16	67.87	70.26	73.65	77.70	80.53

Standard uncertainty u is u(χ_{eff})=1.390 J·cm^{-3}; u(T)=0.10 K; u(P)=0.26 kPa.
[a]p_i: inlet pressure, p_o: outlet pressure

7 was examined, it was seen that all probes were poor solvents for NBA LC since the χ_{eff} values were extremely high.

3. The Separation of Isomers

With the IGC method, it is possible to separate various isomer series from each other. According to this method, the separation of isomers is due to the efficient selectivity of the LC because of its molecular arrangement. The selectivity of the LC for various types of structural isomers is determined by the term "α", which is also expressed as the separation factor or the selectivity coefficient. This term can be calculated as follows [54]:

$$\alpha=\frac{(t_{R1}-t_A)}{(t_{R2}-t_A)}=\frac{V_{g1}^o}{V_{g2}^o} \quad (9)$$

Here, t_{R1} and t_{R2} are the retention time of the first and second isomers from the isomer pairs, respectively, t_A is the retention time of air, V_{g1}^o and V_{g2}^o are the specific retention volume of the first and

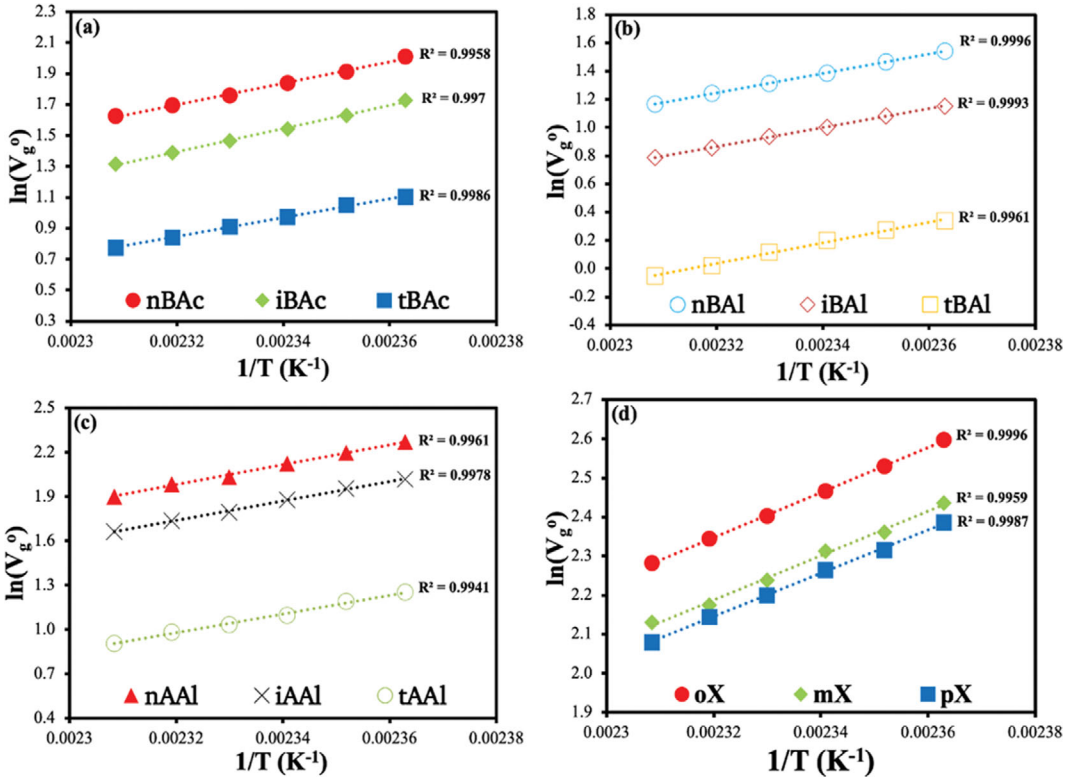

Fig. 5. The retention diagram of isomer series on NBA LC: (a) butyl acetate series, (b) butyl alcohol series, (c) amyl alcohol series, and (d) xylene series.

Table 8. The selectivity coefficients of NBA LC for the isomer pairs: n-butyl acetate (nBAc)/iso-butyl acetate (iBAc), n-butyl acetate (nBA)/tert-butyl acetate (tBAc), n-butyl alcohol (nBAl)/iso-butyl alcohol (iBAl), n-butyl alcohol (nBAl)/tert-butyl alcohol (tBAl), n-amyl alcohol (nAAl)/iso-amyl alcohol (iAAl), n-amyl alcohol (nAAl)/tert-amyl alcohol (tAAl), *o*-Xylene (oX)/*m*-Xylene (mX), and *o*-Xylene (oX)/*p*-Xylene (pX) (423.15-433.15 K)

	Selectivity coefficient ($\alpha = V^o_{g1}/V^o_{g2}$)							
Temperature (K)	nBAc/iBAc	nBAc/tBAc	nBAl/iBAl	nBAl/tBAl	nAAl/iAAl	nAAl/tAAl	*o*X/*m*X	*o*X/*p*X
423.15	1.33	2.48	1.48	3.31	1.29	2.77	1.18	1.24
425.15	1.33	2.38	1.47	3.31	1.27	2.73	1.18	1.24
427.15	1.34	2.37	1.47	3.27	1.28	2.80	1.16	1.22
429.15	1.34	2.33	1.45	3.31	1.27	2.72	1.18	1.23
431.15	1.36	2.35	1.47	3.39	1.28	2.73	1.19	1.22
433.15	1.36	2.35	1.46	3.38	1.27	2.71	1.17	1.23
433.15*	1.34	2.46	1.51	2.99	1.30	2.75	-	-

* The separation coefficients of OBA LC at 433.15 K [42]. Standard uncertainty u is u(α)=0.01; u(T)=0.10 K; u(P)=0.26 kPa.

second isomer pairs calculated according to Eq. (1), respectively. The magnitude of the "α" value indicates the separation ability of the LC. The greater the "α" value than 1, the more effectively LC can separate isomers. If this value is less than 1, separation of isomers is not possible [45].

In this study, the retention behaviors of butyl acetate, butyl alcohol, amyl alcohol, and xylene isomer series were passed over the stationary phase and their V^o_g values were calculated with the help of Eq. (1). Linear retention diagrams (Fig. 5) were drawn between 1/T and lnV^o_g values using these V^o_g values. Then, "α" values were calculated for nBAc/iBAc, nBAc/tBAc, nBAl/iBAl, nBAl/tBAl, nAAl/iAAl, nAAl/tAAl, oX/mX, and oX/pX isomer pairs with the help of Eq. (9) and listed in Table 8. When Table 8 is examined, "α" values greater than 1 indicate that the isomers are separated effectively. Considering all these results, it can be said that NBA LC is very effective in the separation of structural isomers and isomer mixtures. Moreover, "α" values obtained at 433.15 K were compared with the values obtained in our previous study [42]. Using NBA LC, it was seen that the best separation was in the nBAl/tBAl, nAAl/tAAl, and nBAc/tBAc isomer pairs. When all the results were analyzed, it was seen that the isomer separation using NBA and OBA LCs did not depend on the number of -CH_2 groups in

the structure.

CONCLUSION

The thermodynamic characterization of LCs and the determination of their thermodynamic parameters are extremely important in terms of their industrial use and contribution to the literature. In this study, the thermodynamic characterization of the NBA LC was carried out effectively and its thermodynamic parameters were determined by the IGC method, which is easy to apply, low cost, and provides high accuracy results. According to the χ_{12}^{∞}, χ_{12}^{*}, and χ_{eff} values, the non-polar and polar probes used in the study were found to be poor solvents for NBA LC. Besides, according to these parameters and enthalpy values, the solubility of NBA LC in non-polar and polar probes was found to be exothermic. The Flory-Huggins parameters of NBA LC were compared with that of OBA LC in our previous study. According to the results obtained, it was determined that the solubility decreased as the number of -CH_2 in the LC structure increased, at least in this study. In this study, the separation of some series of isomers using NBA LC was also investigated and it was determined that the isomers were effectively separated.

ACKNOWLEDGEMENTS

This research has been supported by Yildiz Technical University Scientific Research Projects Coordination Department. Project number: FDK-2020-4071.

SUPPORTING INFORMATION

Additional information as noted in the text. This information is available via the Internet at http://www.springer.com/chemistry/journal/11814.

REFERENCES

1. J. G. An, S. Hina, Y. Yang, M. Xue and Y. Liu, *Rev. Adv. Mater. Sci.*, **44**, 398 (2016).
2. F. P. Caglar, H. Akdas-Kilic, H. Ocak and B. B. Eran, *J. Mol. Struct.*, **1220**, 128755 (2020).
3. M. Sargazi, M. R. Linford and M. Kaykhaii, *Crit. Rev. Anal. Chem.*, **49**, 243 (2019).
4. D. Andrienko, *J. Mol. Liq.*, **267**, 520 (2018).
5. S. Kumar, R. Verma, A. Dwivedi, R. Dhar and A. Tripathi, *AIP Conf. Proc.*, **1953**, 050014 (2018).
6. D. Sunil, A. A. A. Salam, R. K. Sinha, L. D. Rodrigues, K. Swamynathan and P. Bhagavath, *J. Mol. Liq.*, **335**, 116202 (2021).
7. S. Kumar, R. Verma, R. Dhar and A. Tripathi. *Liq. Cryst.*, **46**, 356 (2019).
8. J. F. Gamble, R. N. Davé, S. Kiang, M. M. Leane, M. Tobyn and S. S. Y. Wang, *Int. J. Pharm.*, **445**, 39 (2013).
9. W. Wang, Q. Wang, J. Tang, Q. Wang and B. Wang, *J. Chem. Thermodyn.*, **150**, 106236 (2020).
10. V. Ugraskan, B. Isik, O. Yazici and F. Cakar, *J. Chem. Eng. Data*, **65**, 1795 (2020).
11. E. Díaz, S. Ordóñez, A. Vega and J. Coca, *Thermochim. Acta*, **434**, 9 (2005).
12. T. V. M. Sreekanth, S. Ramanaiah, P. Reddi Rani and K. S. Reddy, *Polym. Bull.*, **63**, 547 (2009).
13. M. Romansky and J. E. Guillet, *Polymer*, **35**, 584 (1994).
14. O. Yazici, *Chromatographia*, **79**, 355 (2016).
15. P. Wu, S. Qi, N. Liu, K. Deng and H. Nie, *J. Elastom. Plast.*, **43**, 369 (2011).
16. G. S. Dritsas, K. Karatasos and C. Panayiotou, *J. Chromatogr. A*, **1216**, 8979 (2009).
17. F. Mutelet and J. N. Jaubert, *J. Chromatogr. A*, **1102**, 256 (2006).
18. C. L. Young, *Chromatogr. Rev.*, **10**, 129 (1968).
19. A. J. B. Cruickshank, M. L. Windsor and C. L. Young, *Proc. Royal Soc. A Math. Phys. Eng. Sci.*, **295**, 271 (1966).
20. J. R. Conder and J. H. Purnell, *Trans. Faraday Soc.*, **64**, 1505 (1968).
21. Z. Witkiewicz, *J. Chromatogr. A*, **466**, 37 (1989).
22. Z. Witkiewicz, J. Szulc and R. Dábrowski, *J. Chromatogr. A*, **315**, 145 (1984).
23. E. Ghanem and S. Al-Hariri, *Chromatographia*, **77**, 653 (2014).
24. A. E. Cakar, F. Cakar, H. Ocak, S. Karavelioglu, B. B. Eran and O. Cankurtaran, *J. Mol. Struct.*, **1265**, 133379 (2022).
25. I. Erol, F. Cakar, H. Ocak, H. Cankurtaran, O. Cankurtaran, B. Bilgin-Eran and F. Karaman, *Liq. Cryst.*, **43**, 142 (2016).
26. O. Cankurtaran and F. Yilmaz, *Polymer*, **37**, 3019 (1996).
27. M. Tejaswi, P. Pardhasaradhi, B. T. P. Madhav, M. C. Rao, D. R. S. Reddy, G. Giridhar and R. K. N. R. Manepalli, *Optik*, **219**, 165151 (2020).
28. A. J. Herbert, *Trans. Faraday Soc.*, **63**, 555 (1967).
29. M. K. Kozłowska, U. Domańska, M. Lempert and M. Rogalski, *J. Chromatogr. A*, **1068**, 297 (2005).
30. J. Camacho, E. Díez, G. Ovejero and I. Díaz, *J. Appl. Polym. Sci.*, **128**, 481 (2013).
31. I. Gutiérrez, E. Díaz, A. Vega, S. Ordóñez, A. Guerrero-Ruiz, E. Castillejos-López and I. Rodríguez-Ramos, *Thermochim. Acta*, **602**, 36 (2015).
32. N. Karakehya and C. Bilgic, *Int. J. Adhes. Adhes.*, **51**, 140 (2014).
33. S. Sun and J. C. Berg, *Adv. Colloid Interface Sci.*, **105**, 151 (2003).
34. A. Voelkel, B. Strzemiecka, K. Milczewska and Z. Okulus, *Open Chem.*, **13**, 893 (2015).
35. A. L. Revelli, F. Mutelet, J. N. Jaubert, M. Garcia-Martinez, L. M. Sprunger, W. E. Acree and G. A. Baker, *J. Chem. Eng. Data*, **55**, 2434 (2010).
36. A. C. Adiguzel, B. Korkmaz, F. Cakar, O. Cankurtaran and B. F. Senkal, *Fluid Phase Equilib.*, **559**, 113467 (2022).
37. D. G. Gray, *Prog. Polym. Sci.*, **5**, 1 (1977).
38. T. E. Daubert, *Physical and thermodynamic properties of pure chemicals: data compilation*, Hemisphere Publication Corporation, New York (1989).
39. A. F. M. Barton, *Chem. Rev.*, **75**, 731 (1975).
40. J. Klein and H. E. Jeberien, *Die Makromol. Chem.*, **181**, 1237 (1980).
41. C. P. Callaway, K. Hendrickson, N. Bond, S. M. Lee, P. Sood and S. S. Jang, *ChemPhysChem*, **19**, 1655 (2018).
42. B. Isik, F. Cakar, H. Cankurtaran and O. Cankurtaran, *Instrum. Sci. Technol.*, **50**, 1 (2022).
43. K. Schotsch and B. A. Wolf, *Die Makromol. Chem.*, **185**, 2169 (1984).
44. F. Cakar and O. Cankurtaran, *Polym. Bull.*, **55**, 95 (2005).

45. B. Isik, F. Cakar and O. Cankurtaran, *Sep. Sci. Technol.*, **57**, 2843 (2022).
46. D. H. Everett, *Trans. Faraday Soc.*, **61**, 1637 (1965).
47. A. J. B. Cruickshank, B. W. Gainey, C. P. Hicks, T. M. Letcher, R. W. Moody and C. L. Young, *Trans. Faraday Soc.*, **65**, 1014 (1969).
48. J. E. Guillet, M. Romansky, G. J. Price and R. V. D. Mark, *Inverse gas chromatography, characterization of polymers and other materials*, American Chemical Society (1989).
49. Y. Yampolskii and N. Belov, *Macromolecules*, **48**, 6751 (2015).
50. S. Mutlu Yanic, F. Cakar, H. Ocak, F. Karaman, O. Cankurtaran and B. Bilgin Eran, *J. Chem. Eng. Data*, **64**, 1007 (2019).
51. M. Królikowski, M. Królikowska, M. Więckowski and A. Piłowski, *J. Chem. Therm.*, **147**, 106117 (2020).
52. U. Domańska, M. Karpińska and M. Wlazło, *J. Chem. Therm.*, **121**, 112 (2018).
53. O. Cankurtaran and F. Yilmaz, *Polym. Int.*, **41**, 307 (1996).
54. D. W. Katja, *Theory of gas chromatography*, Springer-Verlag (2014).

Supporting Information

Thermotropic liquid crystalline 4-(Nonyloxy) benzoic acid: Phase transition temperatures, thermodynamic characterization, and separation of structural isomers

Birol Isik, Fatih Cakar, Husnu Cankurtaran, and Ozlem Cankurtaran†

Department of Chemistry, Faculty of Arts & Sciences, Yildiz Technical University, Esenler, Istanbul, 34220, Turkey
(*Received 17 January 2023 • Revised 24 May 2023 • Accepted 1 June 2023*)

Table S1. Characteristics of the chemicals used in this study

Chemical name	Chemical formula	CAS	Source	Assay	Molecular weight (g/mol)
4-(Nonyloxy) benzoic acid (NBA)	$CH_3(CH_2)_8OC_6H_4CO_2H$	15872-43-2	Sigma Aldrich	³0.970	264.36
n-Hexane (Hx, C6)	$CH_3(CH_2)_4CH_3$	110-54-3	Supelco	³0.997	86.18
n-Heptane (Hp, C7)	$CH_3(CH_2)_5CH_3$	142-82-5	Supelco	³0.990	100.20
n-Octane (O, C8)	$CH_3(CH_2)_6CH_3$	111-65-9	Sigma Aldrich	³0.990	114.23
n-Nonane (N, C9)	$CH_3(CH_2)_7CH_3$	111-84-2	Sigma Aldrich	³0.990	128.26
n-Decane (D, C10)	$CH_3(CH_2)_8CH_3$	124-18-5	Sigma Aldrich	³0.990	142.28
n-Undecane (UD, C11)	$CH_3(CH_2)_9CH_3$	1120-21-4	Sigma Aldrich	³0.990	156.31
n-Dodecane (DD, C12)	$CH_3(CH_2)_{10}CH_3$	112-40-3	Sigma Aldrich	³0.990	170.33
n-Tridecane (TD, C13)	$CH_3(CH_2)_{11}CH_3$	629-50-5	Sigma Aldrich	³0.990	184.36
Ethyl benzene (EB)	$C_6H_5C_2H_5$	100-41-4	Sigma Aldrich	³0.998	106.17
Ethyl acetate (EA)	$CH_3COOC_2H_5$	141-78-6	Sigma Aldrich	³0.998	88.11
n-Propyl benzene (nPB)	$C_6H_5CH_2CH_2CH_3$	103-65-1	Sigma Aldrich	³0.980	120.19
iso-Propyl benzene (iPB)	$C_6H_5CH(CH_3)_2$	98-82-8	Sigma Aldrich	³0.980	120.19
Chlorobenzene (CB)	C_6H_5Cl	108-90-7	Sigma Aldrich	³0.990	112.56
Toluene (T)	$C_6H_5CH_3$	108-88-3	Sigma Aldrich	³0.998	92.14
n-Butyl acetate (nBAc)	$CH_3COO(CH_2)_3CH_3$	123-86-4	Sigma Aldrich	³0.995	116.16
iso-Butyl acetate (iBAc)	$CH_3COOCH_2CH(CH_3)_2$	110-19-0	Sigma Aldrich	³0.980	116.16
tert-Butyl acetate (tBAc)	$CH_3COOC(CH_3)_3$	540-88-5	Sigma Aldrich	³0.990	116.16
n-Butyl alcohol (nBAl)	$CH_3(CH_2)_3OH$	71-36-3	Sigma Aldrich	³0.994	74.12
iso-Butyl alcohol (iBAl)	$(CH_3)_2CHCH_2OH$	78-83-1	Sigma Aldrich	³0.990	74.12
tert-Butyl alcohol (tBAl)	$(CH_3)_3COH$	75-65-0	Sigma Aldrich	³0.990	74.12
n-Amyl alcohol (nAAl)	$CH_3(CH_2)_4OH$	71-41-0	Sigma Aldrich	³0.990	88.15
iso-Amyl alcohol (iAAl)	$(CH_3)_2CHCH_2CH_2OH$	123-51-3	Supelco	³0.990	88.15
tert-Amyl alcohol (tAAl)	$CH_3CH_2C(CH_3)_2OH$	75-85-4	Sigma Aldrich	³0.990	88.15
o-Xylene (*o*X)	$C_6H_4(CH_3)_2$	95-47-6	Supelco	³0.990	106.17
m-Xylene (*m*X)	$C_6H_4(CH_3)_2$	108-38-3	Sigma Aldrich	³0.990	106.17
p-Xylene (*p*X)	$C_6H_4(CH_3)_2$	106-42-3	Sigma Aldrich	³0.990	106.17

Standard uncertainty u is u(T)=0.1 K; u(P)=0.26 kPa.